HHS Public Access

Author manuscript

Cell Rep. Author manuscript; available in PMC 2020 November 11.

Published in final edited form as:

Cell Rep. 2020 October 27; 33(4): 108306. doi:10.1016/j.celrep.2020.108306.

Epigenetic Mechanisms Contribute to Evolutionary Adaptation of Gene Network Activity under Environmental Selection

Xinyue Luo[1,2,6], **Ruijie Song**[2,3,6], **David F. Moreno**[1,2], **Hong-Yeoul Ryu**[4,7], **Mark Hochstrasser**[1,4], **Murat Acar**[1,2,3,5,8,*]

[1]Department of Molecular Cellular and Developmental Biology, Yale University, 219 Prospect Street, New Haven, CT 06511, USA

[2]Systems Biology Institute, Yale University, 850 West Campus Drive, West Haven, CT 06516, USA

[3]Interdepartmental Program in Computational Biology and Bioinformatics, Yale University, 300 George Street, Suite 501, New Haven, CT 06511, USA

[4]Department of Molecular Biophysics and Biochemistry, Yale University, 266 Whitney Avenue, New Haven, CT 06520, USA

[5]Department of Physics, Yale University, 217 Prospect Street, New Haven, CT 06511, USA

[6]These authors contributed equally

[7]Present address: School of Life Sciences, BK21 Plus KNU Creative BioResearch Group, College of National Sciences, Kyungpook National University, Daegu 41566, Republic of Korea

[8]Lead Contact

SUMMARY

How evolution can be facilitated by epigenetic mechanisms has received refreshed attention recently. To explore the role epigenetic inheritance plays in evolution, we subject isogenic wild-type yeast cells expressing P_{GAL1}-YFP (yellow fluorescent protein) to selection by daily sorting based on reporter expression. We observe expression-level reductions in multiple replicates sorted for the lowest expression that persist for several days, even after lifting the selection pressure. Reduced expression is due to factors in the galactose (GAL) network rather than global factors. Results using a constitutively active GAL network are in overall agreement with findings with the

*Correspondence: murat.acar@yale.edu.

AUTHOR CONTRIBUTIONS

X.L., R.S., and M.A. designed the experiments and analyses, interpreted the data and results, and designed and prepared the manuscript. X.L. constructed the strains, performed the experiments, collected the data, and contributed to data analysis. R.S. analyzed the data and performed statistical analyses. X.L., H.-Y.R., and M.H. performed the ChIP-qPCR experiments and helped interpret their results. D.F.M. performed the mating and sporulation experiments, including strain construction; flow-cytometry measurements and analyses; and interpreting, plotting, and writing the results with M.A. D.F.M. also contributed to the revision of the manuscript. M.H. dissected the tetrads. M.A. conceived and supervised the project. All authors read and approved the manuscript.

DECLARATION OF INTERESTS

The authors declare no competing interests.

SUPPLEMENTAL INFORMATION

Supplemental Information can be found online at https://doi.org/10.1016/j.celrep.2020.108306.

wild-type network. We find that the local chromatin environment of the reporter has a significant effect on the observed phenotype. Genome sequencing, chromatin immunoprecipitation (ChIP)-qPCR, and sporulation analysis provide further insights into the epigenetic and genetic contributors to the expression changes observed. Our work provides a comprehensive example of the role played by epigenetic mechanisms on gene network evolution.

In Brief

Luo et al. demonstrate how epigenetic mechanisms contribute to the evolution of gene network activity. Subjecting yeast cells to repeated environmental selection based on the activity of the galactose network, they observe sustained changes in reporter expression level. They characterize the epigenetic and genetic factors contributing to the observed phenotypes.

Graphical Abstract

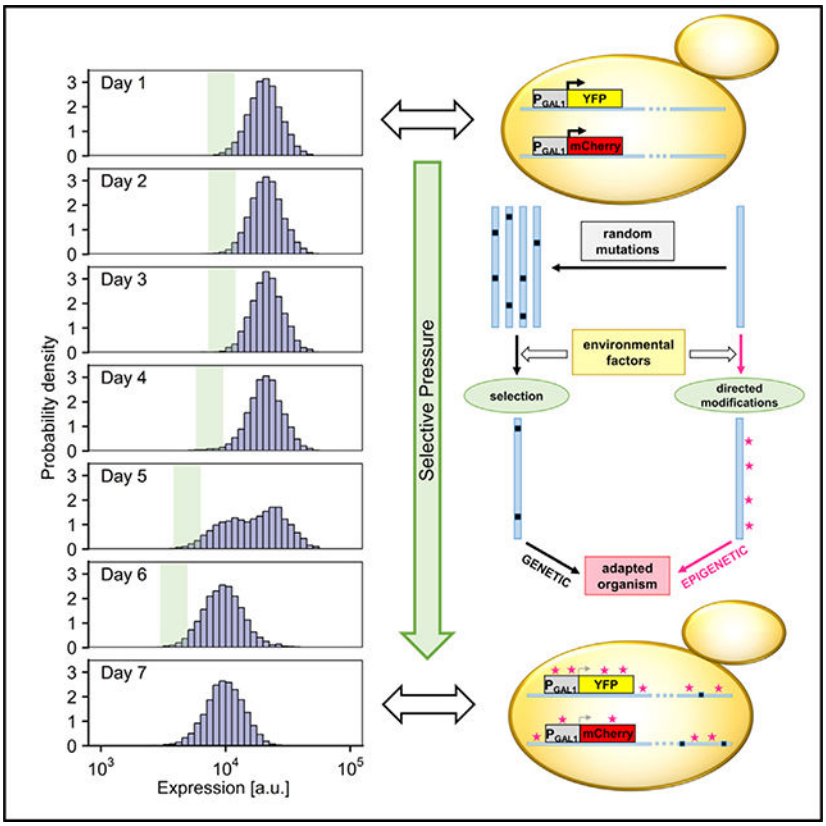

INTRODUCTION

Since Charles Darwin published *On the Origin of Species* in 1859, the concept of evolution by natural selection has occupied a prominent place in modern biology (Darwin, 1859). Darwin himself, of course, had no knowledge of the molecular details of this process: DNA would not be established as the genetic material for another 85 years (Avery et al., 1944). The neo-Darwinian evolution theory combines modern knowledge of genetics and molecular biology with Darwin's thinking (Olson-Manning et al., 2012), but classic neo-Darwinian

evolution theory is focused on genetics as the primary molecular mechanism and has substantial difficulties with the fact that beneficial genetic mutations occur at an extremely low rate (Day and Bonduriansky, 2011; Jablonka and Raz, 2009; Kuzawa and Thayer, 2011; Nei and Nozawa, 2011), to the point where some evolutionary biologists have called for a rethinking of the entire evolutionary theory (Laland et al., 2014).

The concept of inheritance of acquired characteristics is frequently attributed to Lamarck (Skinner, 2015), though perhaps inaccurately (Burkhardt, 2013). Nonetheless, the so-called neo-Lamarckian theory, grounded on epigenetic mechanisms, has received increased attention recently (Burggren, 2014; Day and Bonduriansky, 2011; Skinner et al., 2015). A key postulate of the neo-Lamarckian theory is that environment directly alters phenotype generationally (Figure 1A) (Skinner, 2015). In this context, epigenetic mechanisms can be the mediator for the environment to directly alter phenotypic variation and its subsequent inheritance (Skinner, 2015).

Evolutionary consequences of epigenetic inheritance have been studied in recent years, showing how epigenetic control of gene expression affects adaptation (Bódi et al., 2017; Bonduriansky and Day, 2009; Bonduriansky et al., 2012; Halfmann et al., 2012; Klironomos et al., 2013; Kronholm and Collins, 2016; Stajic et al., 2019). Nongenetic inheritance can be mediated in several ways, such as by the inheritance of epigenetic states, cytoplasmic factors, and nutrients (Bonduriansky and Day, 2009). Nongenetic inheritance and its evolutionary implications have been conceptualized in a general framework, showing that by decoupling phenotypic change from the genotype, nongenetic inheritance could circumvent the limitations of genetic inheritance (Bonduriansky and Day, 2009). Nongenetic and genetic inheritance mechanisms are not mutually exclusive. For example, theoretical predictions suggested that nongenetic inheritance could increase the rate of both phenotypic and genetic change (Bonduriansky et al., 2012). Also, theoretical and computational work showed how the interplay of heritable epigenetic changes with genetic changes could affect adaptive evolution (Klironomos et al., 2013) and how the effect of epigenetic mutations on adaptive walks depended on their stability and fitness effects relative to genetic mutations (Kronholm and Collins, 2016).

In addition to this theoretical work, experimental studies further focused on the evolutionary consequences of nongenetic heterogeneity and inheritance across generations (Acar et al., 2005, 2008; Bódi et al., 2017; Chatterjee and Acar, 2018; Halfmann et al., 2012; Huang, 2009; Peng et al., 2015; Stajic et al., 2019; Tyedmers et al., 2008; Xue and Acar, 2018a, 2018b). For example, yeast prion proteins can act as epigenetic elements of inheritance (Halfmann et al., 2012), and it has been hypothesized that the yeast prion [*PSI*$^{+}$] provides a mechanism to increase survival in fluctuating environments (Tyedmers et al., 2008); it has also been shown that prions are a common mechanism for phenotypic inheritance in wild strains of *Saccharomyces* (Halfmann et al., 2012). In another experimental study focusing on heterogeneity, it has been shown that phenotypic heterogeneity facilitates adaptive evolution, with the heterogeneity being an evolving trait when populations are under chronic selection pressure (Bódi et al., 2017). As the final example, when tuning low, intermediate, and high levels of heritable silencing of a reporter under selection by insertion within silent

subtelomeric yeast chromatin, epigenetic gene silencing has been found to alter the mechanisms and rate of evolutionary adaptation (Stajic et al., 2019).

The concepts of epigenetic inheritance and memory are tightly linked and often used interchangeably to refer to non-DNA-based inheritance (Bonduriansky and Day, 2009). While epigenetic inheritance refers to the passage of certain epigenetic marks to the offspring (Lacal and Ventura, 2018), epigenetic memory is defined as the process of establishing and maintaining a heritable transcriptional state (Acar et al., 2005; Kaufmann et al., 2007; Kundu et al., 2007). Work from the van Oudenaarden group (Acar et al., 2005) described transcriptional memory in the yeast galactose (GAL) network by showing that yeast cells "remember" whether they were previously exposed to high or low concentrations of galactose. Using an engineered GAL network (Acar et al., 2005) where single yeast cells switch between "on" and "off" states of the network, another study (Kaufmann et al., 2007) from the same group measured inheritance of the dynamic gene-expression state and found that several generations after cells have separated, many closely related cell pairs switched with high degrees of synchrony. Providing mechanistic insights into the mediation of epigenetic memory in the GAL network, one study (Kundu et al., 2007) showed that the rate of transcriptional induction of *GAL1* was regulated by the prior expression state; the epigenetic state was inherited by daughter cells, and the SWI/SNF chromatin remodeling enzyme was essential for *GAL1* epigenetic memory. Another study (Brickner et al., 2007) demonstrated that the yeast *GAL1* gene is recruited to the nuclear periphery upon transcriptional activation, and it remains at the periphery for generations after it is repressed, with localization at the periphery serving as a form of memory of recent transcriptional activation. Finally, Tzamarias and colleagues (Zacharioudakis et al., 2007) further showed that the residual activity of the *GAL1*-encoded galactokinase preserves memory in progeny cells by rapidly turning on the Gal4p activator upon cells' re-exposure to galactose.

Despite these studies, a comprehensive example of the role played by neo-Lamarckian epigenetic mechanisms on evolution in the context of a gene network has been lacking. Here, we directly explore the role epigenetic inheritance plays in short-timescale microevolution. We subjected yeast cells to repeated environmental selection based on the expression level of a fluorescent protein reporting on the activity of the canonical GAL network (Figure 1D) (Acar et al., 2005, 2008, 2010; Elison et al., 2018; Luo et al., 2018) over a period of 7 days. We observed reductions in expression level in multiple replicates sorted for the lowest expression that persisted even after the selection pressure was lifted. Using whole-genome sequencing (WGS), chromatin immunoprecipitation (ChIP)-qPCR experiments, and sporulation analysis, we characterized the epigenetic and genetic factors contributing to the persistent expression-level reductions observed.

RESULTS

Applying Environmental Selection on WT GAL Network Activity

To explore the role epigenetic inheritance (Bintu et al., 2016; Bird, 2002; Kouzarides, 2007; Li and Zhang, 2014; Zhou et al., 2011) may play in short-timescale microevolution, we designed an experiment in which a population of isogenic wild-type (WT) yeast cells expressing the yellow fluorescent protein (YFP) under the *GAL1* promoter is subjected to

repeated environmental selection in the form of daily sorting based on the expression level of the reporter as measured by flow cytometry. During a 7-day period and corresponding to approximately 101 generations with a 100-min doubling time, the cells were sorted daily based on YFP expression level, and only cells whose expression level is within a particular range (either the lowest 5%, the middle 5%, or the highest 5%; Figure 1E) were selected and allowed to grow further in the same environment (Figures 1B and 1C).

Immediately after sorting, the expression-level distribution of the selected cells is extremely narrow, and it gradually relaxes over time, either to the original distribution if the sorting procedure had no lasting effect on the expression level or to a different distribution with different statistical properties (Figure 1C). By monitoring the expression-level distributions over the 7-day sorting period, one can discern if the sorting intervention had any impact on the expression of the reporter. To determine if any change in the reporter expression observed was transient or lasting, immediately after the 7-day sorting period, the population was grown 3 additional days free from selection pressure to see if the expression-level distribution reverted back to the original after the selection pressure was lifted.

We found no significant expression-level changes in cells sorted for the middle or highest expression levels (Figure 2B). It is unsurprising that cells already at the middle expression levels retained their character. Given the already high expression levels from the *GAL1* promoter, the lack of change in the cells sorted for the highest expression level may be simply because there is little room for it to increase further. On the other hand, all 12 biological replicates sorted for the lowest expression levels displayed marked reduction in expression (Figures 2A and 2B) to varying degrees that persisted during the 3-day selection-free growth period. Nine replicates were grown (free of selection) for a further 16 days (approximately 230 generations), and 8 of the 9 retained the expression-level reduction (Figure 2C).

To better understand the possible causes driving the observed expression-level reduction, we introduced a second fluorescent reporter protein, mCherry, into the cells. We constructed two strains in which mCherry was either driven by the *TEF1* promoter or the *GAL1* promoter and performed the same YFP-sorting experiment on these strains. We found no change in the expression level of mCherry in the P_{TEF1}-mCherry strain (Figure S1) but significant reduction in the mCherry expression level in the P_{GAL1}-mCherry strain (Figure 3). Further, the level and timing of mCherry expression-level reduction in the P_{GAL1}-mCherry strain was synchronized with that of YFP (Figure 3C). We therefore conclude that the observed reduction in expression was likely due to some factor specific to the GAL network rather than a global factor that can be expected to also affect the expression from P_{TEF1}-mCherry.

Dissecting System Behavior in the Constitutively Active GAL Network

The natural GAL network contains a number of interacting regulators forming feedback loops (Acar et al., 2010; Peng et al., 2016). This complicates the interpretation of the results. For example, the synchronized reduction in double-reporter expression could be due to the dynamics of the epigenetic regulation of the *GAL1* promoter activity, or it could be due to the upstream regulatory elements in the WT GAL network. To eliminate such complication, we deleted the *GAL80* gene—which codes for a repressor through which other GAL

network regulators exert their effects—effectively converting the P_{GAL1} promoter into a constitutive promoter dependent only on the transcription factor Gal4p (Figure 4A) and repeated the YFP-sorting experiments in this strain. A total of nine biological replicates were used, two of which were found to have accumulated mutations in *GAL4* or the reporter during the course of the experiment and were excluded from further analysis (Data S1).

We found that most biological replicates in which the cells were sorted for the lowest-YFP-expressing cells continued to display a downward shift in mean YFP expression level, although the extent of the shift varied from replicate to replicate, and in one replicate there was no significant change (Figures 4B and 4C, blue curves); five replicates were further grown free of selection for 8 additional days (approximately 115 generations), and all retained their reduced expression levels during this selection-free period (Figures 4E and 4F). Cells sorted for the middle or highest YFP expression did not display any significant changes in either YFP or mCherry expression (Figures 4B and 4C, green and pink curves), just like WT cells. Measuring the doubling times of the cells belonging to colonies isolated from the biological replicate that displayed the largest downward shift in YFP expression (~70%) showed a small increase in doubling times for five colonies isolated from the 7th-day culture, compared to the selection-free positive control (Figure S2A).

We also observed a downward shift in mCherry expression level despite sorting cells in the YFP channel. In all but one of the biological replicates, the YFP and mCherry expression levels were in agreement, but in one replicate, the level of expression-level reduction was significantly different (Figure 4D), though the timing of reduction was similar. This suggests that at least two underlying mechanisms are in play. One mechanism affects the *GAL1* promoter activity generally, driving the synchronized behavior seen both here and previously (Figure 3). But another mechanism, apparently specific to the P_{GAL1}-YFP reporter, must exist that drives the divergence in expression-level reduction between the two reporters, as seen in the last biological replicate.

Measuring Noise Dynamics under Environmental Selection

To see how the selection pressure potentially influences the expression heterogeneity, we next examined the level of noise in P_{GAL1}-YFP and P_{GAL1}-mCherry expression when *gal80Δ* cells were sorted throughout the 7-day period. We discerned no change in the level of P_{GAL1}-YFP noise (coefficient of variation [CV]) in the positive control (no gating) sample or when cells were sorted for the middle or highest expression (Figure S3A).

However, we observed an increase in noise in several samples when cells were sorted for the lowest expression (Figure S3A, blue). Like the change in the expression level itself, this noise increase was stable when the cells were grown selection-free for an additional 10 days after the 7-day sorting period (Figures S3C and S3D, blue). Moreover, in two samples, an accompanying increase in P_{GAL1}-mCherry noise can be seen when cells were sorted for the lowest P_{GAL1}-YFP expression (Figures S3A–S3D). Under the extreme selection pressure applied during the sorting process, it is unsurprising that higher levels of noise in the protein whose expression is under selection (YFP) may prove evolutionarily beneficial (by increasing the number of cells having reduced expression levels and hence selected during the sorting process). On the other hand, it is likely not advantageous to have higher noise in

the expression level of mCherry—or, as a proxy, the structural genes of the *GAL* network, which are responsible for metabolizing the GAL taken from the static environment. Diverging from the optimal level of *GAL* network expression in the environment carries a fitness cost (and higher noise means that more cells are diverging from the optimal level), which could explain why the noise level does not display the same degree of synchronization behavior as the expression-level reduction.

The Effect of the Local Chromatin Environment on Observed Results

To understand the potential influence of genomic loci on the level of expression-level reduction, we performed the same sorting experiment but based on the expression level of P_{GAL1}-mCherry (which was integrated into the *ura3* locus) rather than P_{GAL1}-YFP (which was in the *ho* locus). A total of nine biological replicates were used, two of which were found to have accumulated mutations in *GAL4* or the reporter during the experiment and were excluded from further analysis. Measuring the resulting *GAL1* promoter activity levels during the 7-day sorting period as before, we found expression-level reduction to be significantly more difficult to achieve (Figures 5A–5C), if not impossible, compared to sorting when the reporter cassette is integrated into the *ho* locus, with only one biological replicate out of seven displaying a significant reduction in expression compared to the positive control. We similarly quantified the level of noise in P_{GAL1}-YFP and P_{GAL1}-mCherry expression during these mCherry-sorting experiments (Figures 5D and 5E). We did not detect substantial and persistent changes in noise levels of the kind we had seen previously (Figures S3A and S3B).

Together, these observations suggest that the genomic locus at which the cassette is integrated, and hence the local chromatin structure and epigenetic markers, has a significant effect on the phenotype we observed. The *ho* locus appears to be significantly more susceptible to experiencing expression-level reduction in response to the selection pressure we applied compared to the *ura3* locus. Especially given that the genetic mutation rate appears to be approximately constant between the two experiments (in both cases, two out of nine biological replicates were found to have accumulated mutations in the relevant genes), the diverging outcomes strongly suggests that a non-genetic mechanism is involved in suppressing the YFP expression at the *ho* locus.

As noted, sequencing detected no mutations in *GAL4* or the two reporter cassettes (totaling approximately 8 kbp) in the biological replicates under consideration. In addition, we did not detect any substantial fitness changes in the sorted populations passed from one day to the next; if anything, the sorted populations divide slightly slower than unsorted cells (Figure S2). We therefore hypothesized that the observed downward shifts in expression level were due to epigenetic changes in the transcription factor gene *GAL4* and/or in the reporter promoters: the accumulated epigenetic changes “lock” the chromatin into a closed state and are enriched by the daily sorting process. Given the experimental observations, such locks were then necessarily strong enough to persist through hundreds of generations of selection-free growth.

WGS to Explore Genetic Causes of Observed Phenotypes

Next, we performed WGS to evaluate any contributions from global genetic factors on the observed reduction in YFP expression levels. For this, we focused on two biological replicates—the FL6 and FL9 populations in the *gal80Δ* background (STAR Methods)—from which we had seen significant reduction in P_{GAL1}-YFP and P_{GAL1}-mCherry expression on Day7, compared to Day0 expression levels, after gated sorting in the YFP channel. Our local sequencing of the Day7 FL6 and FL9 populations in the reporter cassettes and the *GAL4* region did not identify any mutations.

We isolated five single colonies from the FL6 and FL9 populations on Day7 and randomly selected two single colonies from each of the two groups for performing WGS on them. As controls, we also included in these WGS characterizations two randomly selected single colonies isolated from the Day0 population, as well as two randomly selected single colonies isolated from the positive control group on Day7. Results obtained from the sequencing of each isolated colony were compared to those obtained from the sequencing of the Day0 colonies (Data S2, S3, and S4). While mutations in intergenic promoter regions may also have phenotypic consequences, for the sake of interpretability, we focused on the SNPs (single-nucleotide polymorphisms) causing amino acid alterations in open reading frames (ORFs). We then selected the common ORF mutations found in both single colonies isolated from the FL6 and FL9 populations. Five common mutations were identified for the FL6 colonies (in *FEN2*, *GPM2*, *IRA2*, *NUP133*, and *RPN4*), while the FL9 colonies shared three mutations (in *APL1*, *BDS1*, and *SRB8*).

To see the isolated effects of these mutations on the P_{GAL1}-YFP and P_{GAL1}-mCherry expression levels, we attempted to clone them singly and in combination into a single colony isolated from the unevolved Day0 population using CRISPR. For the FL6 group mutations, we successfully cloned the mutations in the *FEN2*, *IRA2*, and *NUP133* genes one at a time and combinatorically, but the mutations in the *GPM2* and *RPN4* genes could not be cloned because of challenges associated with CRISPR. Measuring the P_{GAL1}-YFP and P_{GAL1}-mCherry expression levels in each constructed strain, we did not see any major changes in expression levels caused by the mutations in *FEN2*, *IRA2*, or *NUP133* genes relative to the Day0 isogenic background without these mutations (Figure S4A). Regarding the mutations in the *GPM2* and *RPN4* genes that could not be cloned, *GPM2* is a nonfunctional homolog of *GPM1* phosphoglycerate mutase, and *RPN4* codes for a transcription factor that stimulates expression of proteasome genes. Despite the potential relevance of *RPN4* for the phenotypes we observed, the degradation experiments we performed for the colonies isolated from the FL6 population did not show differential degradation dynamics for YFP or mCherry (Figures S5A and S5B). Nevertheless, we cannot fully exclude the possibility that the mutations in *GPM2* and/or *RPN4* might exert effects on the phenotypes we observed if they were cloned into the Day0 unevolved, single-colony-derived population.

For the mutations on the *APL1*, *BDS1*, and *SRB8* genes of the FL9 group, on the other hand, we combinatorically constructed all eight strains carrying these mutations one at a time and together. Measuring the P_{GAL1}-YFP and P_{GAL1}-mCherry expression levels in each constructed strain, we saw consistent changes in P_{GAL1}-YFP and P_{GAL1}-mCherry expression levels, relative to the Day0 isogenic background without the mutations (Figure

S4B). The degradation experiments we performed for the colonies isolated from the FL9 population did not show differential degradation dynamics for YFP or mCherry (Figures S5C and S5D). The mutation in *SRB8*, coding for a subunit of the RNA polymerase II (RNA Pol II) mediator complex, led to 75% and 50% reductions in the P_{GAL1}-YFP and P_{GAL1}-mCherry expression levels, respectively, across all strains carrying the mutation. Since these expression reductions in levels of YFP and mCherry are very similar to the ones observed at the end of the 7-day sorting period, the mutation in the *SRB8* gene can account for the phenotypic changes observed in one of the biological replicates (sorting group FL9). However, the differential effects of the *SRB8* mutation on YFP and mCherry expression levels indicate that integration-locus-specific epigenetic factors still play a role on the main phenotype of gene expression reduction under environmental selection.

Measuring Acetylation and Methylation Levels on System Components

To further investigate the effect of epigenetic factors on the difference in expression-level decrease between the two reporters as a result of the *SRB8* mutation, we examined the chromatin modification levels at the *GAL4*, *GAL1*, P_{GAL1}-YFP, and P_{GAL1}-mCherry loci in the two WGS-characterized isogenic colonies of the FL9 group (FL9_2 and FL9_5), as well as isogenic colonies isolated from the Day0 population and Day7 positive control population. For this, we tested for three different types of histone modifications via ChIP-qPCR: trimethylation of histone H3 lysine 4 (H3K4me3), which positively correlates with transcriptional activity; trimethylation of histone H3 lysine 36 (H3K36me3), which represses transcription and is known to be associated with HDAC (Histone DeACetylase) recruitment; and acetylation of histone H3 lysine 27 (H3K27ac), which is associated with active transcription.

As expected based on the YFP and mCherry expression levels, ChIP-qPCR results from the Day0 and Day7 positive control colonies showed higher overall H3K4me3 and H3K27Ac levels but lower H3K36me3 levels, compared to the results observed from the FL9_2 and FL9_5 colonies (Figures 6A–6C; Table S1). More specifically, at the endogenous *GAL1* locus, we saw reductions in H3K4me3 and H3K27Ac levels and an increase in H3K36me3 level in the FL9_2 and FL9_5 colonies, compared to the Day7 positive control colony, suggesting that the local transcriptional activities at the *GAL1* locus in FL9_2 and FL9_5 are lower than in Day0 and Day7 positive control. This is consistent with other observations: in FL9_2 and FL9_5, the YFP protein level was reduced significantly (approximately 70% reduction compared to the Day7 positive control), and there was a significant decrease in the mRNA level of YFP as quantified by qRT-PCR (Figures S6 and S7). We also observed a comparable trend of change in the epigenetic marks at the P_{GAL1}-YFP reporter, indicating that the three types of chromatin modifications tested are similar on these two genetic elements and that both loci are likely governed by the same epigenetic modification machineries that act on the *GAL1* promoter.

We did not see a clear difference between the FL9 colonies and the Day0 and Day7 control colonies at the *GAL4* locus with respect to the H3K36me3 and H3K27Ac modifications, although there seemed to be some reduction of the H3K4me3 mark in FL9_2 and FL9_5.

We interpret this as a consequence of a lack of local chromatin-repressing machinery, considering that *GAL4* is expressed constitutively.

Interestingly, while we observed similar trends in H3K36me3 and H3K27Ac modifications at P_{GAL1}-mCherry compared to *GAL1* and P_{GAL1}-YFP, we saw no differentiating trend in the H3K4me3 modification among the tested colonies at P_{GAL1}-mCherry. This divergence suggests a difference in the local chromatin dynamics between the two reporters. It is possible that the locus where P_{GAL1}-mCherry is placed, *URA3* on chromosome V, has a distinct local chromatin regulatory mechanism that interferes with *GAL1*-promoter-specific regulation. The lack of the H3K4me3 mark at P_{GAL1}-mCherry relative to P_{GAL1}-YFP suggests that transcriptional activity at the former is higher than the latter. Indeed, while YFP protein level in FL9_2 and FL9_5 on Day7 was reduced by 70% relative to Day0, mCherry protein level was reduced by only 50%. Therefore, the difference in expression reduction between the two reporters is associable with the difference in the local chromatin modification levels between the two loci where they are located. Together, these results solidify the role of epigenetic modifications on the expression levels of the two reporters.

Sporulation-Based Assessment of Genetic versus Epigenetic Contributions on the Observed Phenotypes

To rule out the possibility that the observed phenotypes of the evolved strains could be explained on purely genetic grounds, we crossed our evolved strains (FL6_2 and FL9_2) with the equivalent of our unevolved WT strain (Day0) of opposite mating type. As a control, we crossed two unevolved WT strains of opposite mating type. After mating, sporulation, and tetrad dissection, we measured the YFP and mCherry expression levels displayed by the progeny of each cross after growing the cells in the same media conditions as used during our evolution experiments. As expected, all offspring of the WT-to-WT cross showed expression levels very similar to the parental strain (Figure 7A).

The FL6_2-to-WT cross generated offspring that was very heterogeneous in expression, contrary to what would be expected from plausible Mendelian genetic mechanisms (Figure 7B). Moreover, the lack of offspring clustering around the parental FL6_2 strain suggested that the mutations on *GPM2* and *RPN4* were not relevant to the observed phenotypes; were they relevant, Mendelian genetics would predict that half (or a quarter) of the offspring spores would carry the mutations on one (or both) of those genes and display a similar phenotype to that of the parental strain, but the fraction of the spores displaying a similar phenotype to that of the parental strain was actually much lower. Surprisingly, a substantial fraction of the spores displayed reporter expression levels higher than the WT parental strain's expression, especially for the YFP reporter. While there was some correlation (Pearson's r = 0.697) between the YFP and mCherry expression levels, we saw that some spores displayed YFP levels higher than the WT but mCherry levels closer to the level displayed by the evolved FL6_2's low mCherry expression level. Meiosis and sporulation are complex cellular programs involving the creation and repair of double-strand breaks on the DNA in certain recombination hotspots (Kolodkin et al., 1986; Lichten and Goldman, 1995; Smith and Nicolas, 1998), and it is known that epigenetic state influences the meiotic recombination hotspots (Brachet et al., 2012). Therefore, a potential explanation for these

expression levels is that epigenetic changes carried by the evolved parental strain might have caused unusual meiotic recombination events in the offspring.

The offspring generated from the FL9_2-to-WT cross displayed three clearly distinct clusters of YFP and mCherry expression: one coincided with the parental WT strain's reporter expressions, one coincided with the parental FL9_2 strain's expressions, and the third cluster displayed a WT-like YFP expression and a FL9_2-like mCherry expression (Figure 7C). The reporter expression composition of the third cluster would not be expected based on a purely genetic inheritance pattern, as all genetic components controlling the network are the same for both reporters. Since the only difference between the two genetic constructs (P_{GAL1}-YFP and P_{GAL1}-mCherry) is their chromosomal integration site, we attribute the differential gene expression to the differential impact of the epigenetic marks between the YFP and the mCherry loci, as we described in the previous section.

To explain these three expression clusters displayed by the offspring of the FL9_2-to-WT cross, we propose a model in which the mutation in the RNA Pol II mediator subunit Srb8 contributes to the reporter's downregulation, but epigenetic marks at the YFP reporter locus make its expression level independent of which *SRB8* allele the cell is carrying (Figure 7D), potentially through an epigenetically facilitated compensation mechanism maintaining the overall progression of RNA Pol II irrespective of the Srb8 subunit activity. The inheritance pattern we observed from the offspring of the FL9_2-to-WT crossing supports the presence of epigenetic modifications leading to WT-like YFP expression in one of the three expression clusters. More specifically, the parental FL9_2 strain, which bears both the *SRB8* mutated allele and differential epigenetic marks at the YFP insertion locus (Figures 6A and 6C), displays low YFP and mCherry expression (Figure 7C); the unevolved strain bearing the mutated *SRB8* allele in a WT-like chromatin environment also displays low YFP and mCherry expression (Figure S4B). Therefore, the epigenetic mark we are proposing to explain the offspring's third cluster should favor WT-like YFP expression, as only this inheritance model would generate a 3:1 inheritance pattern for the YFP expression and a 2:2 pattern for the mCherry expression, which matches our observations (Figures 7E and 7F).

Overall, these results indicate that the mechanism behind the observed expression reduction during our evolution experiments cannot be explained only by genetic causes. Epigenetic modifications must be contributing to the differential expression pattern exhibited by the two reporters within the same cell and to the overall evolved phenotype emerging at the end of the evolution process.

DISCUSSION

In this report, we explored the role epigenetic inheritance plays in short-timescale microevolution. We observed reductions in expression level in multiple replicates sorted for the lowest expression that persisted for hundreds of generations, long after the selection pressure was lifted. The amount of decrease in expression level was locus specific, implicating the involvement of local chromatin environment in the process. Performing WGS characterizations on isogenic colonies obtained from two populations, we found that one case of the persistent expression-level reduction was due to genetic factors, while

experiments performed for the other case did not indicate a genetic contributor. Measuring the level of chromatin modification marks on system components supported the conclusion that epigenetic regulation differences between integration loci could explain differential YFP and mCherry expression under the same promoter. Finally, results from mating and sporulation experiments provided evidence for the involvement of non-genetic inheritance mechanisms as contributors to the differential expression pattern exhibited by the two reporters in the same cell.

For the replicate that is guided mainly genetically, given that a single mutation in the *SRB8* gene is sufficient to reproduce the decreased YFP and mCherry protein levels measured on Day7, a plausible explanation for this could be that the impaired mRNA synthesis machinery led to a loss in mRNA production and subsequently in protein production in the cell. Since Srb8 is involved in global RNA synthesis, one would expect a global reduction in mRNA levels in the cell as well. We indeed saw a significant reduction in the mRNA level of the housekeeping *ACT1* gene (Figure S7A). Moreover, we found that the isogenic colonies isolated from the FL9 group had significantly increased doubling time compared to both Day0 (~3% increase) and Day7 positive controls (~4% increase), revealing a reduced fitness level that is potentially attributable to inefficient mRNA synthesis. Despite the genetic contributions to the observed phenotypes, we note that crossing and sporulation analysis showed that the inheritance pattern of this strain's traits was not explainable by a solely genetic mechanism.

Our study involves observation of YFP and mCherry expression dynamics with reporter constructs integrated in different genomic loci. We note that genomic loci differ not only in their local chromatin environment, but also in their sequence context (e.g., presence or absence of certain enhancers), which may be a contributor to expression-level differences between the reporters.

Genetic and epigenetic mechanisms do not have to be mutually exclusive. In response to a particular environmental condition, both kinds of mechanisms can play roles and complement each other. Epigenetic mechanisms generally operate at a shorter timescale than genetic mechanisms, allowing a faster response to changing environmental conditions (Bonduriansky et al., 2012; Burggren, 2016). On the other hand, genetic mechanisms operate at a longer timescale but also produce a more permanent response.

To test whether short-term epigenetic inheritance interacts with genetic change, a recent study (Stajic et al., 2019) used an experimental evolution setup in yeast by tuning low, intermediate, and high levels of heritable silencing of a *URA3* reporter under selection. The authors showed that heritable gene expression through epigenetic chromatin states contributed to adaptive evolution; however, their results and interpretations were not free from mutational effects. More specifically, heritable silencing drove population size expansion and rapid epigenetic adaptation, eventually leading to genetic assimilation of the silent phenotype by mutations. Also, at intermediate or low levels of heritable silencing, the study showed that populations evolved more rapidly by accumulation of adaptive mutations.

Natural environments are usually not fully static, but they fluctuate over time. Memory of previous expression levels, from whatever source, can function as a double-edged sword in fluctuating environments. On one hand, having some memory of the optimal expression level in the current environment confers a fitness advantage in the present (Brickner et al., 2007; Zacharioudakis et al., 2007). On the other hand, locking the expression at a particular level would prevent the cell from responding to environmental changes. Thus, fully persistent memory of expression level would be expected to be detrimental in a fluctuating external environment (Acar et al., 2008; Bódi et al., 2017).

Of the various kinds of heritable factors, genetic mutations are certainly among the most persistent; the cell is full of mechanisms aiming to ensure that genetic materials are faithfully passed from one generation to the next, and moreover, reverting a genetic mutation naturally is even more difficult given the randomness of the mutagenesis process and the rarity of gain-of-function mutations. However, epigenetic mechanisms of reducing gene expression are likely easier to revert when the environment demands it (Klironomos et al., 2013); after all, chromatin is routinely remodeled during the cell cycle (Deniz et al., 2016; Raynaud et al., 2014). Thus, compared to genetic mechanisms, the wide variety of epigenetic mechanisms of regulating gene expression levels are much more easily tuned to environmental demands. While some epigenetic changes may disappear within a few generations (Kundu et al., 2007), others can be highly persistent (Catania et al., 2020). Thus, the epigenetic toolset allows the cell to strike a balance between memorizing gene expression states and being plastic to external environmental changes.

STAR★METHODS

RESOURCE AVAILABILITY

Lead Contact—Requests for further information and for resources and reagents should be directed to and will be fulfilled by the Lead Contact, Murat Acar (murat.acar@yale.edu).

Materials Availability—Yeast strains and plasmids used in this study are described in the Key Resources Table and will be made available upon request from the Lead Contact, Murat Acar (murat.acar@yale.edu).

Data and Code Availability—The accession numbers for the sequencing data from WGS runs reported in this paper are GenBank: SAMN11440943, GenBank: SAMN11440944, GenBank: SAMN11440945, GenBank: SAMN11440946, GenBank: SAMN11440947, GenBank: SAMN11440948, GenBank: SAMN11440949, GenBank: SAMN11440950. These numbers are also listed in the Key Resources Table.

EXPERIMENTAL MODEL AND SUBJECT DETAILS

***Saccharomyces* cerevisiae with the W303 genetic background—**All yeast *Saccharomyces* cerevisiae strains constructed are based on the haploid W303 strain background. Complete genotypic descriptions of all strains can be found in the Key Resources Table.

All cultures were grown in synthetic minimal media with histidine dropout and appropriate supplements of other amino-acids. Culture growths were performed in a 30°C shaker (225rpm) in a volume of 1mL. After 48hrs of growth on histidine-dropout minimal media plates containing 2% glucose, strains were grown in liquid minimal media for 22hr ("overnight") in the presence of 0.1% mannose as a non-inducing sole carbon source. This was followed by a 72hr induction period in liquid minimal media containing 0.1% mannose and 0.2% galactose as carbon sources.

METHOD DETAILS

Construction of yeast strains and plasmids—Strains used to study the GAL network were built on WP35 which is a haploid wild-type strain carrying single copy of the P_{GAL1}-*YFP* reporter in the *ho* locus. The double reporter strains carrying a second reporter (P_{GAL1}-*mCherry-tCYC1* or P_{TEF1}-*mCherry-tCYC1*) were constructed with the following steps. First, plasmids carrying P_{GAL1}-*mCherry-tCYC1* or P_{TEF1}-*mCherry-tCYC1* on the pRS306 backbone (Sikorski and Hieter, 1989) were constructed using the Gibson Assembly® Master Mix and NEBuilder® Assembly Tool (New England BioLabs). The resulting plasmids were then linearized within the *URA3* gene at BstBI cut site and transformed into WP35 using the standard lithium acetate (LiOAc) transformation technique. qPCR was performed to select colonies carrying single copy of the second reporter. To obtain the strain XLUYmCgΔ80, the P_{AgTEF}-*natNT2-tADH1* cassette from pYM17 (Euroscarf, Janke et al., 2004) was integrated into the double reporter strain carrying P_{GAL1}-*YFP-tCYC1* and P_{GAL1}-*mCherry-tCYC1* to replace the *GAL80* gene by using 60bps homology regions immediately before and after *GAL80*.

For the mating and sporulation experiments, a MATa counterpart for XLUYmCgΔ80 strain was constructed, starting with the MA0002 strain. First, a single copy of *HIS5*-P_{GAL1}-*YFP-tCYC1* was inserted into the *ho* locus by using 60bp homology regions around the *ho* locus. Then, the P_{GAL1}-*mCherry-tCYC1* plasmid was linearized by BstBI and inserted in single-copy into the *URA3* locus. Finally, the *GAL80* ORF was deleted by amplifying the P_{AgTEF}-*KanR-tAgTEF1* cassette from the *pFA6-kanMX4* plasmid (Wach et al., 1994) with 60bp homology regions immediately before and after the *GAL80* ORF.

Flow cytometry data acquisition and sorting—After the induction period described in the "Experimental Model and Subject Details" section above, the expression distribution of ~50,000 cells were measured by flow cytometry (FACS-Aria; Becton Dickinson) at flow rates between 4 to 8 (flow rate scale of 1–11 corresponds to approximately 10–80 μL/min), and the cell-sorting period was initiated. During the 7-day-long sorting period, populations underwent expression-based sorting once a day, followed by the selection-free growth period lasting from 3 to 20 days during which the entire expression distribution was passed from one day to the next instead of gated-sorting. Every 24hrs during the 7-day-long gated-sorting period, individual cells were sorted into fresh media of the same type by applying fluorescence intensity based gates rendering the highest, middle and lowest 4.8%–5.2% of the total cell population (referred to as HIGH, MID, LOW). In "forward" sorting groups, the gates were selected based on YFP fluorescence, while in the "reverse" sorting groups they were selected based on mCherry fluorescence. 450 individual cells were sorted for the HIGH

groups, and 600 cells were sorted for all other groups. To minimize potential variations in the size and/or morphology of the sorted cells, the gating process also involved applying a narrow FSC-SSC (ForwardSCatter-SideSCatter) range corresponding to the densest ~20% of the total cell population. Grown cultures taken from Day0, Day7, the last day of the selection-free period, as well as certain other days throughout each sorting period were frozen on the same day for further analysis. Starting from the overnight growth period and until the end of the gated and selection-free sorting periods, cell densities were kept low (between OD_{600} 0.2 and 0.3) to prevent nutrient depletion.

mRNA transcript levels determination by qRT-PCR—Selected cell populations of the strain XLUYmCgΔ80 frozen after sorting on Day0 and Day7 were recovered as single isogenic colonies from glycerol stocks streaked on 2% glucose minimal media plates with histidine dropout. Colonies were then grown overnight in liquid minimal media containing 0.1% mannose as the sole carbon source, and induced in minimal media containing 0.1% mannose and 0.2% galactose for 48hrs in 50mL volume, reaching a final OD_{600} of less than 0.2. Fluorescence levels of the induced cells were recorded by flow cytometry right before harvesting for total RNA. cDNA was prepared by using the High Capacity RNA-to-cDNA kit from Applied Biosystems. The resulting cDNA was then used in qPCR reactions to quantify mRNA levels of genes of interest. For qPCR, we used the iTaq™ Universal SYBR® Green Supermix from Bio-Rad and targeted 4 genes with 2 sets of primers for each: ACT1 (primer pair EPIACT1–2F and EPIACT1–2R were used as the endogenous control for ΔC_T calculation), YFP, mCherry, GAL1, and GAL4. The relative transcription levels for samples within the same sorting experimental group were calculated with the Day0 population's transcript levels used as the control. The qPCR primers used are listed on Table S2. The amplicons were between 158 and 161bps long.

Local sequencing of key GAL network components—To see whether or not mutations were accumulated on the genetic components relevant to the GAL network activity, frozen cell populations from Day0 and Day7 sorting groups of the strain XLUYmCgΔ80 (the groups that showed at least 20% decrease in YFP or mCherry expression compared to corresponding Day0 expression) were recovered from glycerol stocks streaked on 2% glucose minimal media plates with histidine dropout. Populations were then grown overnight in liquid minimal media containing 0.1% mannose as the sole carbon source, and induced in minimal media containing 0.1% mannose and 0.2% galactose for 48hrs in 1mL volume, reaching a final OD_{600} of less than 0.3. After the induction period, expression measurements were performed by flow cytometry and also genomic DNA contents were extracted from the induced populations to sequence key genetic components of the GAL network. All re-induced Day7 populations exhibited similar expression levels relative to expression levels of their corresponding Day0 populations; in other words, freezing and re-induction after the actual sorting process did not alter the relative expression levels in these populations. For sequencing, we selected the LOW ("L") sorting groups of the strain XLUYmCgΔ80 which showed over 20% decrease in reporter expression; the local sequencing was performed for the P_{GAL1}-YFP, P_{GAL1}-mCherry, and P_{GAL4}-GAL4 constructs from the beginning of the promoters to the end of the terminators. With "F or R" indicating "Forward or Reverse" sorting based on YFP or mCherry, these Day7 sequenced

groups of sorted populations were named as FL1, FL2, FL6, FL8, FL9, RL2, RL5, and RL6; the numbers indicate the identity of the biological replicate from the 7-day-long sorting experiment. Sequencing was first performed on the population level for these sorting groups; genomic DNA was prepared from the entire sorted populations from Day7, and no apparent mutation was identified. Then, 5 randomly-selected single colonies were isolated from each population for isogenic expression characterization, and sequencing was performed on select single colonies which had similar expression profile as the corresponding original population. No mutation on the P_{GAL1}-YFP, P_{GAL1}-mCherry, P_{GAL4}-GAL4 constructs was found in colonies isolated from the FL1, FL6, FL9, RL2, RL5, whose full sequences are given in Data S1; however, mutations/changes were found in colonies isolated from FL2, FL8 and RL6 (Data S1).

Whole Genome Sequencing (WGS) sample preparation—Out of the 5 single colonies isolated from the FL6 and FL9 populations on Day7 (for which local-sequenced for the P_{GAL1}-YFP, P_{GAL1}-mCherry, P_{GAL4}-GAL4 constructs did not identify any mutations), we randomly selected 2 single colonies from each of the FL6 and FL9 groups for performing whole genome sequencing on them. As controls, we also included in these WGS characterizations 2 randomly-selected single colonies isolated from the Day0 population, as well as 2 randomly selected single colony isolated from the positive control group on Day7.

Cells from each single colony were recovered from glycerol stock on 2% glucose minimal media plates with histidine dropout, and grown in 10mL YPD liquid media until the cell-density (OD_{600}) reached ~1. The YeaStar Genomic DNA Kit (ZYMO Research) was used for genomic DNA extraction. The process was repeated 2–3 times until 1–5 μg of purified DNA ($OD_{260/280}$ between 1.8 and 2) concentrated in 50 μL of TE buffer was acquired for each sample. The purified DNA were pooled and sequenced at the Yale Center for Genome Analysis with Illumina HiSeq4000 (paired-end, 150bp) targeting 200X coverage.

Measuring doubling-times of cell populations—Five isogenic colonies isolated from each of the Day7 FL6 and FL9 populations, as well as one isogenic colony isolated from each of the Day0 and Day7 positive controls, were recovered from glycerol stocks and streaked on 2% glucose minimal media plates with histidine dropout. Colonies were then grown overnight in liquid minimal media containing 0.1% mannose as the sole carbon source, and induced in minimal media containing 0.1% mannose and 0.2% galactose for 48hrs in 1mL volume, reaching a final OD_{600} of less than 0.3. Following the induction period, cultures were continuously grown in the same media conditions, and the growth rate analyses were performed based on the dilution rates and the OD_{600} values measured at 6 different time points across the next 52–55hrs. At each time point, all cultures were diluted to maintain OD_{600} below 0.55 to keep growth at log-phase and to prevent nutrition depletion. The average log-phase doubling-time $t_{doubling}$ was calculated (Figures S2A and S2B) using the following formula:

$$t_{doubling} = t_{duration} \Big/ \log_2 \left(\frac{D_{end}}{D_{start}} * \prod_{k=1}^{N} d_k \right)$$

$t_{duration}$: duration between the start and end of the continuous culture growth

D_{end}: OD_{600} at the end of continuous culture growth

D_{start}: OD_{600} at the start of continuous culture growth

N: total number of dilutions (here N = 6)

d_k: dilution rate at time point k

SNP introduction with CRISPR-Cas9—Select mutations identified from WGS were cloned into a single colony from Day0 to see if each or all of them could result in the phenotypic changes observed in the sorting experiment. To choose candidate mutations, we first selected mutations within ORFs that cause changes in their corresponding amino acids. We then selected the common mutations found in both single colonies isolated from a group: 5 common mutations for FL6 (*FEN2*, *GPM2*, *IRA2*, *NUP133, RPN4*), and 3 common mutations for FL9 (*APL1*, *BDS1, SRB8*). To introduce these mutations back into a single colony from Day0, a centromeric plasmid with backbone pRS314 carrying a Cas9 cassette was first transformed into a Day0 single colony. For each mutation, the resulting strain was transformed with donor DNA carrying the mutation together with a plasmid with backbone pRS305 carrying guide RNA cassette targeting the mutation site. The final strains were sequenced locally to verify the intended genetic alterations.

Degradation dynamics of fluorescent proteins—Five isogenic colonies isolated from each of the Day7 FL6 and FL9 populations, as well as one isogenic colony isolated from each of the Day0 and Day7 positive control, were recovered from glycerol stocks and streaked on 2% glucose minimal media plates with histidine dropout. Colonies were then grown overnight in liquid minimal media containing 0.1% mannose as the sole carbon source, and induced in minimal media containing 0.1% mannose and 0.2% galactose for 48hrs, reaching a final OD_{600} of ~0.2 in a total volume of 5mL for each sample. Cycloheximide (Sigma-Aldrich, C7698) was then added to the cultures at the final concentration of 10 μg/mL. Samples were taken from the cycloheximide-treated cultures for fluorescence measurements with flow cytometry (FACS-Aria, Becton Dickinson) at the following time points while the cultures continued being incubated in a 30°C shaker: 0hr (right before adding cycloheximide), 15min (right after adding cycloheximide), 1.5hr, 4hr, 6hr, 21hr and 28.5hr.

During the flow cytometry measurements, due to the cycloheximide treatment, changes were observed in the position of the total cell population based on the FSC-SSC readings. Therefore, a large FSC-SSC gate covering the densest 40%–80% of the total population was applied.

ChIP-qPCR experiments—From the single colonies selected for WGS, we selected the two colonies from FL9 together with one single colony from each of the Day0 and Day7 positive control group for histone modification characterization with ChIP-qPCR. We tested three types of histone modifications at GAL1, GAL4, YFP and mCherry open reading frames: H3K4me3, H3K36me3 and H3Ac. A yeast strain with *set1Δ* background was used

as negative control for the H3K4me3 group. Cells from each single colony were recovered from glycerol stock on 2% glucose minimal media plates with histidine dropout, grown overnight in minimal media containing 0.1% mannose as the sole carbon source, and induced in minimal media containing 0.1% mannose and 0.2% galactose for 48hrs. We used 300mL of culture with OD_{600} ~0.4 to initiate ChIP.

ChIP experiments were performed as described previously (Ahn et al., 2004; Ryu and Ahn, 2014). Briefly, formaldehyde was added to a final concentration of 1% for 20 min. Cross-linking was quenched by addition of glycine to 240 mM. Cells were collected by centrifugation, washed in TBS twice, and then lysed with glass beads in FA lysis buffer {50 mM HEPES-KOH at pH 7.5, 150 mM NaCl, 1 mM EDTA, 1% Triton X-100, 0.1% Na deoxycholate, 0.1% SDS, cOmplete protease inhibitor cocktail (Roche, 11697498001), 1 mM PMSF (AmericanBio, AB01620)}. Sheared chromatin by sonication was incubated with Protein G-Sepharose (GE Healthcare, 17–0618-01) bound with anti-H3K4me3 (Abcam, ab8580), anti-H3K36me3 (Abcam, ab9050), anti-H3Ac (Millipore, 07–360), or anti-H3 (Abcam, ab1791). Following washings, eluted chromatin fragments were treated with pronase (Roche, 11 459 643 001), and DNA was purified by phenol/chloroform extraction. qPCR assays were performed using 1:8 diluted DNA template, and then the results for methylated or acetylated H3 were normalized to total histone H3 signals and the internal control (a fragment amplified from an untranscribed region on ChrIV).

Forward and reverse primer sequences used for ChIP-qPCR are listed on Table S2. EPIYFP pair targets 169–327bp from 5′ of YFP ORF; EPImC-1 pair targets 177–338bp from 5′ of mCherry ORF; EPIGal1–1 pair targets 319–476bp from 5′ of GAL1 ORF; EPIGal4–1 pair targets 2225–2385bp from 5′ of GAL4 ORF; IntIV pair is the endogenous control and targets an intergenic region on chromosome IV.

Mating, sporulation and tetrad dissection—The desired strains were grown in YPD plates overnight. Then, a small amount of the fresh patch of cells was mixed with its mating counterpart in a fresh YPAD plate (YPD supplemented with 20mg/L Ade) and incubated for 4h at 30°C. Zygote formation was checked by microscopy and a portion of the mating patch was transferred to YPD+Nat+G418 plate, which selected for diploid cells. Single diploid colonies were transferred to GNA pre-sporulation plates (Giaever et al., 2002) (5% glucose, 3% nutrient broth, 1% yeast extract, 2% agar) and grown for a day at 30°C, and then transferred to sporulation plates (Kaiser et al., 1994) (1% potassium acetate, 0.1% yeast extract, 0.05% dextrose, 2% agar) where they were incubated at room temperature for 4–5 days. Tetrad dissection was performed on a YPD plate after degrading the ascus wall with β-glucuronidase (Sigma-Aldrich, G7017), and then incubated at 30°C for 2 days. The spores coming from each tetrad were spotted on YPD+G418 and YPD+Nat plates to check that they were displaying a proper segregation pattern of the markers, which qualified them for further analysis.

QUANTIFICATION AND STATISTICAL ANALYSIS

Flow cytometry data analysis—Each sample of flow cytometry (FACSAria, Becton Dickinson) data were analyzed in R using the Bioconductor flowCore software package

(Hahne et al., 2009). The FSC-SSC gate was chosen to cover the densest portion of the total population and eliminate individuals with unusual morphologies, such as dying cells and cell debris; the same gate was used for all samples gathered during a single experiment. Each FACS sample had on average ~7500 cells after gating. Log-amplified fluorescence measurements for the gated cells were converted to linear scale for analysis. When needed for the wild-type strain, a threshold for ON state was selected based on fluorescence measurements from uninduced cells and applied uniformly to all relevant samples.

The raw expression level of each strain on each day during the multi-day experiment is measured by averaging the single-cell reporter fluorescence as measured by flow cytometry. To control for the effect of day-to-day variations, the raw expression levels were normalized using the average expression level of the same reporter in the positive control samples measured on the same day.

Whole Genome Sequencing data analysis—The sequencing reads were first trimmed using Trimmomatic (Bolger et al., 2014) with the following settings: “LEADING:3 TRAILING:3 SLIDINGWINDOW:2:30” (Barbieri et al., 2017). The filtered reads from each sample were independently aligned to the current version of S288C reference genome from Ensembl using BWA-MEM (Li, 2013) and converted to BAM format using SAMtools. Picard’s MarkDuplicates (https://github.com/broadinstitute/picard) was used to mark duplicates in the resulting BAM files. We then realigned the reads with the GATK tools (Van der Auwera et al., 2013) RealignerTargetCreator and IndelRealigner, and variants were called using GATK’s HaplotypeCaller with “-ploidy 1.” SNPs and Indels were extracted from the resulting file and filtered manually using GATK’s SelectVariants and VariantFiltration. For SNP, we used the following parameters: -filterExpression “QD<2.0 || FS>50.0 || MQ<50.0 || SOR>3.0 || MQRankSum<−12.5 || ReadPosRankSum<−8.0.” For Indel, we used these parameters: -filterExpression “QD<2.0 || FS>200.0 || InbreedingCoeff< −0.8 || SOR>10.0 || ReadPosRankSum<−20.0.” Finally, we used VCFtools (Danecek et al., 2011) to identify variants in FL6, FL9 and Day7-positive-control samples relative to Day0, which were then annotated with Ensembl’s VEP tool (McLaren et al., 2016).

χ^2 test for checking inheritance models for sporulation outcomes—The proposed inheritance model was tested as described (Griffiths et al., 2000). Briefly, the χ^2 test statistic was calculated as $\sum_{i=1}^{n} \frac{(E_i - O_i)^2}{E_i}$, where n is the number of classes for a phenotype, E_i is the expected number of individuals under that class according to the model, and O_i is the experimentally-observed number of individuals classified under that class. This test statistic was compared with the χ^2 distribution with n-1 degrees of freedom to obtain the likelihood of the experimental observation if the assumed model was true (p value).

Supplementary Material

Refer to Web version on PubMed Central for supplementary material.

ACKNOWLEDGMENTS

We thank J. Gendron, E. Karatekin, L. Mirny, G.P. Wagner, and Acar Lab members for comments and feedback on various stages of this work. X.L. acknowledges support through the China Scholarship Council-Yale World Scholars Program. M.H. acknowledges funding from the US National Institutes of Health (GM136325). M.A. acknowledges funding from the US National Institutes of Health (1DP2AG050461-01 and 1U54CA209992-01).

REFERENCES

Acar M, Becskei A, and van Oudenaarden A (2005). Enhancement of cellular memory by reducing stochastic transitions. Nature 435, 228–232. [PubMed: 15889097]

Acar M, Mettetal JT, and van Oudenaarden A (2008). Stochastic switching as a survival strategy in fluctuating environments. Nat. Genet. 40, 471–475. [PubMed: 18362885]

Acar M, Pando BF, Arnold FH, Elowitz MB, and van Oudenaarden A (2010). A general mechanism for network-dosage compensation in gene circuits. Science 329, 1656–1660. [PubMed: 20929850]

Ahn SH, Kim M, and Buratowski S (2004). Phosphorylation of serine 2 within the RNA polymerase II C-terminal domain couples transcription and 3′ end processing. Mol. Cell 13, 67–76. [PubMed: 14731395]

Avery OT, Macleod CM, and McCarty M (1944). Studies on the chemical nature of the substance inducing transformation of pneumococcal types: Induction of transformation by a desoxyribonucleic acid fraction isolated from pneumococcus type iii. J. Exp. Med. 79, 137–158. [PubMed: 19871359]

Barbieri EM, Muir P, Akhuetie-Oni BO, Yellman CM, and Isaacs FJ (2017). Precise Editing at DNA Replication Forks Enables Multiplex Genome Engineering in Eukaryotes. Cell 171, 1453–1467.e13. [PubMed: 29153834]

Bintu L, Yong J, Antebi YE, McCue K, Kazuki Y, Uno N, Oshimura M, and Elowitz MB (2016). Dynamics of epigenetic regulation at the single-cell level. Science 351, 720–724. [PubMed: 26912859]

Bird A (2002). DNA methylation patterns and epigenetic memory. Genes Dev. 16, 6–21. [PubMed: 11782440]

Bódi Z, Farkas Z, Nevozhay D, Kalapis D, Lá zár V, Csörgő B, Nyerges Á, Szamecz B, Fekete G, Papp B, et al. (2017). Phenotypic heterogeneity promotes adaptive evolution. PLoS Biol. 15, 1–26.

Bolger AM, Lohse M, and Usadel B (2014). Trimmomatic: a flexible trimmer for Illumina sequence data. Bioinformatics 30, 2114–2120. [PubMed: 24695404]

Bonduriansky R, and Day T (2009). Nongenetic Inheritance and Its Evolutionary Implications. Annu. Rev. Ecol. Evol. Syst. 40, 103–125.

Bonduriansky R, Crean AJ, and Day T (2012). The implications of nongenetic inheritance for evolution in changing environments. Evol. Appl. 5, 192–201. [PubMed: 25568041]

Brachet E, Sommermeyer V, and Borde V (2012). Interplay between modifications of chromatin and meiotic recombination hotspots. Biol. Cell 104, 51–69. [PubMed: 22188336]

Brickner DG, Cajigas I, Fondufe-Mittendorf Y, Ahmed S, Lee PC, Widom J, and Brickner JH (2007). H2A.Z-mediated localization of genes at the nuclear periphery confers epigenetic memory of previous transcriptional state. PLoS Biol. 5, e81. [PubMed: 17373856]

Burggren WW (2014). Epigenetics as a source of variation in comparative animal physiology - or - Lamarck is lookin' pretty good these days. J. Exp. Biol. 217, 682–689. [PubMed: 24574384]

Burggren W (2016). Epigenetic Inheritance and Its Role in Evolutionary Biology: Re-Evaluation and New Perspectives. Biology (Basel) 5, 24.

Burkhardt RW Jr. (2013). Lamarck, evolution, and the inheritance of acquired characters. Genetics 194, 793–805. [PubMed: 23908372]

Catania S, Dumesic PA, Pimentel H, Nasif A, Stoddard CI, Burke JE, Diedrich JK, Cook S, Shea T, Geinger E, et al. (2020). Evolutionary Persistence of DNA Methylation for Millions of Years after Ancient Loss of a De Novo Methyltransferase. Cell 180, 263–277.e20. [PubMed: 31955845]

Chatterjee M, and Acar M (2018). Heritable stress response dynamics revealed by single-cell genealogy. Sci. Adv. 4, e1701775. [PubMed: 29675464]

Danecek P, Auton A, Abecasis G, Albers CA, Banks E, DePristo MA, Handsaker RE, Lunter G, Marth GT, Sherry ST, et al.; 1000 Genomes Project Analysis Group (2011). The variant call format and VCFtools. Bioinformatics 27, 2156–2158. [PubMed: 21653522]

Darwin C (1859). On the origin of species by means of natural selection, or, the preservation of favoured races in the struggle for life (J. Murray).

Day T, and Bonduriansky R (2011). A unified approach to the evolutionary consequences of genetic and nongenetic inheritance. Am. Nat. 178, E18–E36. [PubMed: 21750377]

Deniz Ö, Flores O, Aldea M, Soler-López M, and Orozco M (2016). Nucleosome architecture throughout the cell cycle. Sci. Rep. 6, 19729. [PubMed: 26818620]

Elison GL, Xue Y, Song R, and Acar M (2018). Insights into Bidirectional Gene Expression Control Using the Canonical GAL1/GAL10 Promoter. Cell Rep. 25, 737–748.e4. [PubMed: 30332652]

Giaever G, Chu AM, Ni L, Connelly C, Riles L, Véronneau S, Dow S, Lucau-Danila A, Anderson K, André B, et al. (2002). Functional profiling of the Saccharomyces cerevisiae genome. Nature 418, 387–391. [PubMed: 12140549]

Griffiths AJF, Miller JH, Suzuki DT, Lewontin RC, and Gelbart WM (2000). An Introduction to Genetic Analysis, Seventh Edition (W. H. Freeman).

Hahne F, LeMeur N, Brinkman RR, Ellis B, Haaland P, Sarkar D, Spidlen J, Strain E, and Gentleman R (2009). flowCore: a Bioconductor package for high throughput flow cytometry. BMC Bioinformatics 10, 106. [PubMed: 19358741]

Halfmann R, Jarosz DF, Jones SK, Chang A, Lancaster AK, and Lindquist S (2012). Prions are a common mechanism for phenotypic inheritance in wild yeasts. Nature 482, 363–368. [PubMed: 22337056]

Huang S (2009). Non-genetic heterogeneity of cells in development: more than just noise. Development 136, 3853–3862. [PubMed: 19906852]

Jablonka E, and Raz G (2009). Transgenerational epigenetic inheritance: prevalence, mechanisms, and implications for the study of heredity and evolution. Q. Rev. Biol. 84, 131–176. [PubMed: 19606595]

Janke C, Magiera MM, Rathfelder N, Taxis C, Reber S, Maekawa H, Moreno-Borchart A, Doenges G, Schwob E, Schiebel E, and Knop M (2004). A versatile toolbox for PCR-based tagging of yeast genes: new fluorescent proteins, more markers and promoter substitution cassettes. Yeast 21, 947–962. [PubMed: 15334558]

Kaiser C, Michaelis S, and Mitchell A (1994). Methods in Yeast Genetics: A Cold Spring Harbor Laboratory Course Manual (Cold Spring Harbor Laboratory Press).

Kaufmann BB, Yang Q, Mettetal JT, and van Oudenaarden A (2007). Heritable stochastic switching revealed by single-cell genealogy. PLoS Biol. 5, e239. [PubMed: 17803359]

Klironomos FD, Berg J, and Collins S (2013). How epigenetic mutations can affect genetic evolution: model and mechanism. BioEssays 35, 571–578. [PubMed: 23580343]

Kolodkin AL, Klar AJS, and Stahl FW (1986). Double-strand breaks can initiate meiotic recombination in S. cerevisiae. Cell 46, 733–740. [PubMed: 3527443]

Kouzarides T (2007). Chromatin modifications and their function. Cell 128, 693–705. [PubMed: 17320507]

Kronholm I, and Collins S (2016). Epigenetic mutations can both help and hinder adaptive evolution. Mol. Ecol. 25, 1856–1868. [PubMed: 26139359]

Kundu S, Horn PJ, and Peterson CL (2007). SWI/SNF is required for transcriptional memory at the yeast GAL gene cluster. Genes Dev. 21, 997–1004. [PubMed: 17438002]

Kuzawa CW, and Thayer ZM (2011). Timescales of human adaptation: the role of epigenetic processes. Epigenomics 3, 221–234. [PubMed: 22122283]

Lacal I, and Ventura R (2018). Epigenetic Inheritance: Concepts, Mechanisms and Perspectives. Front. Mol. Neurosci. 11, 292. [PubMed: 30323739]

Laland K, Uller T, Feldman M, Sterelny K, Müller GB, Moczek A, Jablonka E, Odling-Smee J, Wray GA, Hoekstra HE, et al. (2014). Does evolutionary theory need a rethink? Nature 514, 161–164. [PubMed: 25297418]

Li H (2013). Aligning sequence reads, clone sequences and assembly contigs with BWA-MEM. arXiv, arXiv:1303.3997. https://arxiv.org/abs/1303.3997.

Li E, and Zhang Y (2014). DNA methylation in mammals. Cold Spring Harb. Perspect. Biol. 6, a019133. [PubMed: 24789823]

Lichten M, and Goldman ASH (1995). Meiotic recombination hotspots. Annu. Rev. Genet. 29, 423–444. [PubMed: 8825482]

Luo X, Song R, and Acar M (2018). Multi-component gene network design as a survival strategy in diverse environments. BMC Syst. Biol. 12, 85. [PubMed: 30257679]

McLaren W, Gil L, Hunt SE, Riat HS, Ritchie GRS, Thormann A, Flicek P, and Cunningham F (2016). The Ensembl Variant Effect Predictor. Genome Biol. 17, 122. [PubMed: 27268795]

Nei M, and Nozawa M (2011). Roles of mutation and selection in speciation: from Hugo de Vries to the modern genomic era. Genome Biol. Evol. 3, 812–829. [PubMed: 21903731]

Olson-Manning CF, Wagner MR, and Mitchell-Olds T (2012). Adaptive evolution: evaluating empirical support for theoretical predictions. Nat. Rev. Genet. 13, 867–877. [PubMed: 23154809]

Peng W, Liu P, Xue Y, and Acar M (2015). Evolution of gene network activity by tuning the strength of negative-feedback regulation. Nat. Commun. 6, 6226. [PubMed: 25670371]

Peng W, Song R, and Acar M (2016). Noise reduction facilitated by dosage compensation in gene networks. Nat. Commun. 7, 12959. [PubMed: 27694830]

Raynaud C, Mallory AC, Latrasse D, Jégu T, Bruggeman Q, Delarue M, Bergounioux C, and Benhamed M (2014). Chromatin meets the cell cycle. J. Exp. Bot. 65, 2677–2689. [PubMed: 24497647]

Ryu H-Y, and Ahn S (2014). Yeast histone H3 lysine 4 demethylase Jhd2 regulates mitotic rDNA condensation. BMC Biol. 12, 75. [PubMed: 25248920]

Sikorski RS, and Hieter P (1989). A system of shuttle vectors and yeast host strains designed for efficient manipulation of DNA in Saccharomyces cerevisiae. Genetics 122, 19–27. [PubMed: 2659436]

Skinner MK (2015). Environmental epigenetics and a unified theory of the molecular aspects of evolution: A neo-Lamarckian concept that facilitates neo-Darwinian evolution. Genome Biol. Evol. 7, 1296–1302. [PubMed: 25917417]

Skinner MK, Guerrero-Bosagna C, and Haque MM (2015). Environmentally induced epigenetic transgenerational inheritance of sperm epimutations promote genetic mutations. Epigenetics 10, 762–771. [PubMed: 26237076]

Smith KN, and Nicolas A (1998). Recombination at work for meiosis. Curr. Opin. Genet. Dev. 8, 200–211. [PubMed: 9610411]

Stajic D, Perfeito L, and Jansen LET (2019). Epigenetic gene silencing alters the mechanisms and rate of evolutionary adaptation. Nat. Ecol. Evol. 3, 491–498. [PubMed: 30718851]

Tyedmers J, Madariaga ML, and Lindquist S (2008). Prion switching in response to environmental stress. PLoS Biol. 6, e294. [PubMed: 19067491]

Van der Auwera GA, Carneiro MO, Hartl C, Poplin R, del Angel G, Levy-Moonshine A, Jordan T, Shakir K, Roazen D, Thibault J, et al. (2013). From FastQ Data to High-Confidence Variant Calls: The Genome Analysis Toolkit Best Practices Pipeline. Curr. Protoc. Bioinformatics 43, 11.10.1–11.10.33. [PubMed: 25431634]

Wach A, Brachat A, Pöhlmann R, and Philippsen P (1994). New heterologous modules for classical or PCR-based gene disruptions in Saccharomyces cerevisiae. Yeast 10, 1793–1808. [PubMed: 7747518]

Xue Y, and Acar M (2018a). Mechanisms for the epigenetic inheritance of stress response in single cells. Curr. Genet. 64, 1221–1228. [PubMed: 29846762]

Xue Y, and Acar M (2018b). Live-Cell Imaging of Chromatin Condensation Dynamics by CRISPR. iScience 4, 216–235. [PubMed: 30027155]

Zacharioudakis I, Gligoris T, and Tzamarias D (2007). A yeast catabolic enzyme controls transcriptional memory. Curr. Biol. 17, 2041–2046. [PubMed: 17997309]

Zhou VW, Goren A, and Bernstein BE (2011). Charting histone modifications and the functional organization of mammalian genomes. Nat. Rev. Genet. 12, 7–18. [PubMed: 21116306]

Highlights

- Gated sorting and regrowth of low-expression cells causes sustained expression decrease
- Chromatin environment affects expression changes in response to selective pressure
- Genetic causes alone cannot explain the expression reduction under selection
- Inheritance of epigenetic factors contributes to the observed phenotypic change

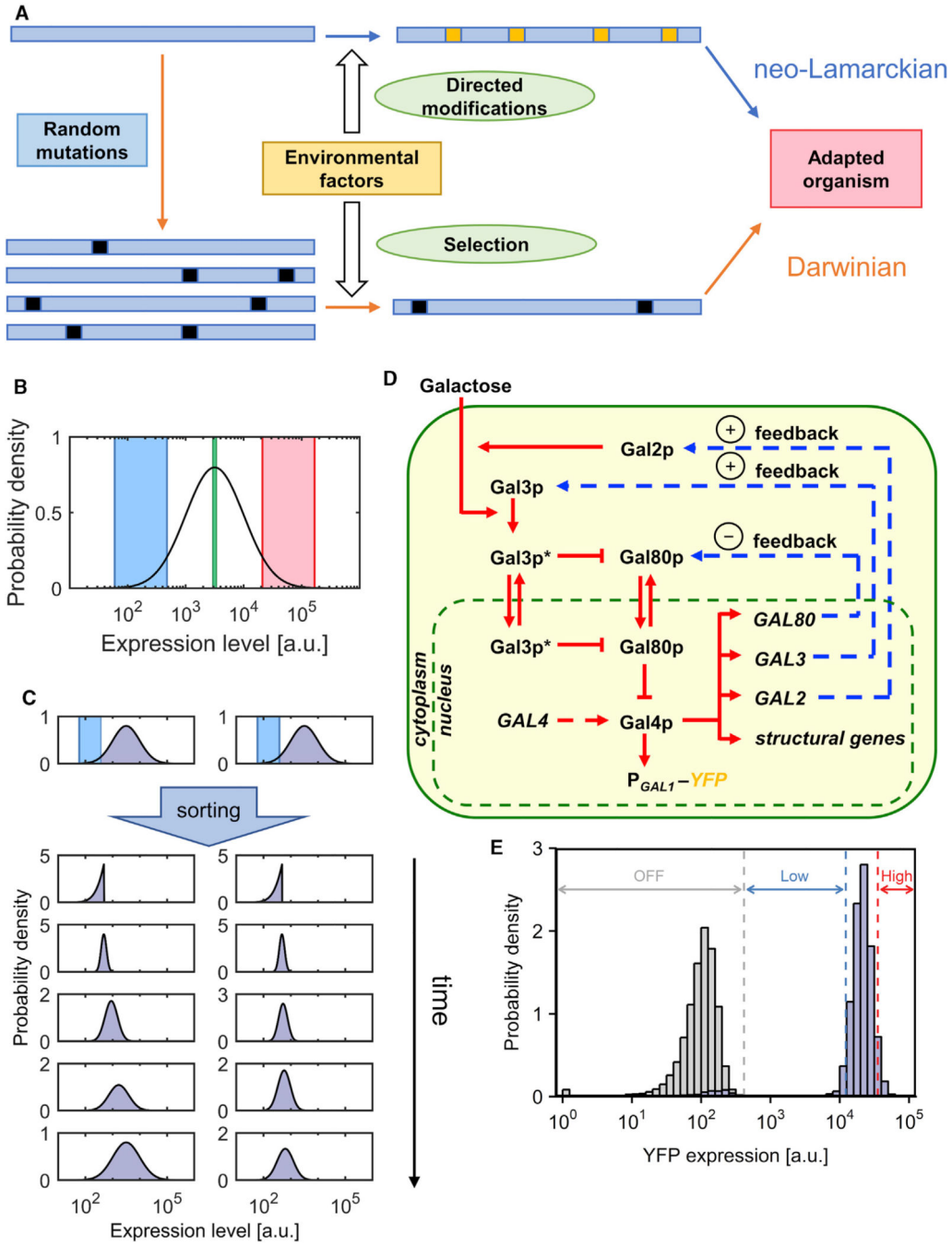

Figure 1. Evolutionary Models, Study Design, and Model Network

(A) Illustration of Darwinian (orange arrows) and neo-Lamarckian (blue arrows) models of evolution. Blue rectangles represent DNA. Black and yellow squares represent genetic mutations and epigenetic modifications, respectively.

(B) Illustration of the three possible sorting gates used: lowest 5% (blue), middle 5% (green), and highest 5% (red).

(C) Illustration of two possible outcomes of the sorting experiment. After being sorted for the lowest-expressing cells, the initial sharp distribution of expression levels will gradually

relax, but it may relax either back to the same distribution as the original (left) or to a different distribution with a lower mean (right).

(D) Gene network architecture of the WT yeast GAL network whose activity is reported using a P_{GAL1}-YFP reporter.

(E) Sorting gate determination for WT cells. The off-peak position is determined using expression data measured from uninduced cells (gray bars); the sorting gates in the induced samples (purple bars) are then selected considering only “on” cells.

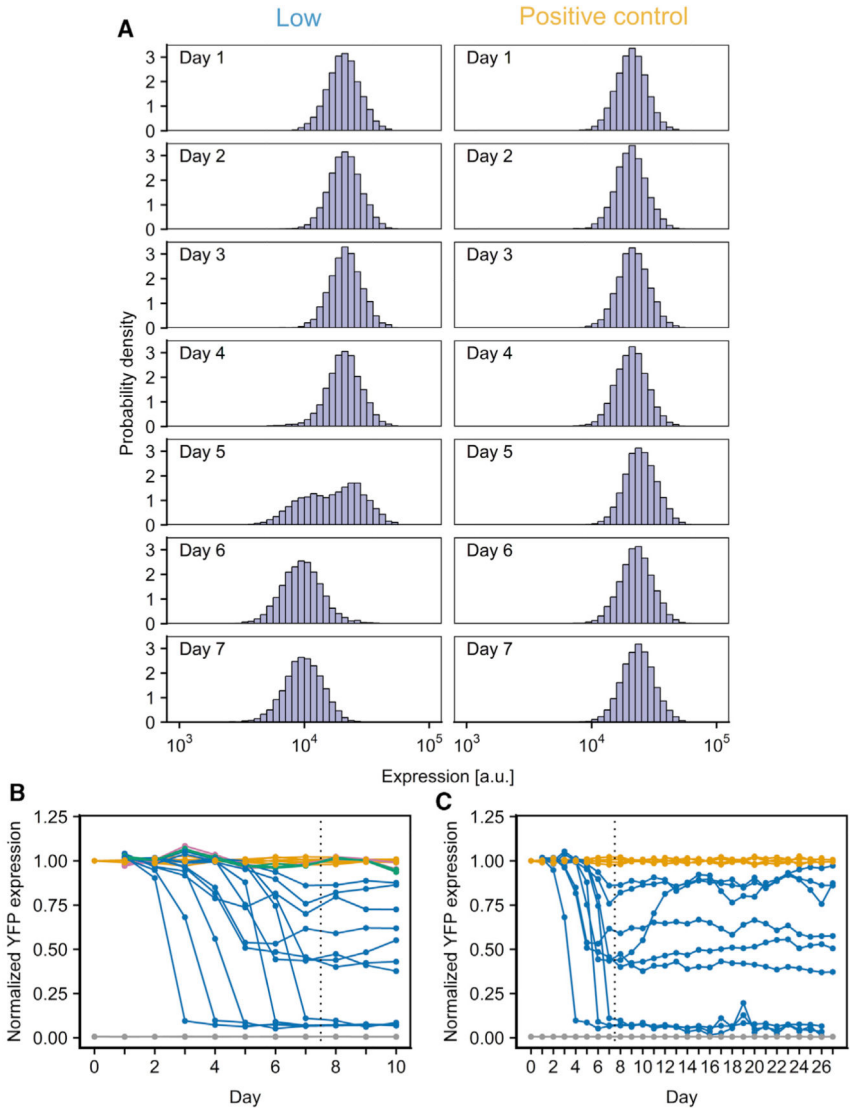

Figure 2. Applying Environmental Selection on WT GAL Network Activity

(A) Sample YFP expression distributions for one of the WT replicates sorted for the lowest expression (left) compared to the positive control (right) over the first 7 days of the experiment.

(B) Normalized YFP expression levels from the YFP-sorting experiment in WT cells. Pink indicates samples sorted for the highest expression, green indicates samples sorted for the median expression, blue indicates samples sorted for the lowest expression, orange indicates positive control, and gray indicates negative control. The dashed line indicates the time at which expression-level-based sorting is terminated. All expression levels are normalized to the corresponding positive control.

(C) Normalized YFP expression levels from the extended YFP-sorting experiment in WT cells. Blue indicates samples sorted for the lowest expression, orange indicates positive control, and gray indicates negative control. The dashed line indicates the time at which expression-level-based sorting is terminated. All expression levels are normalized to the corresponding positive control.

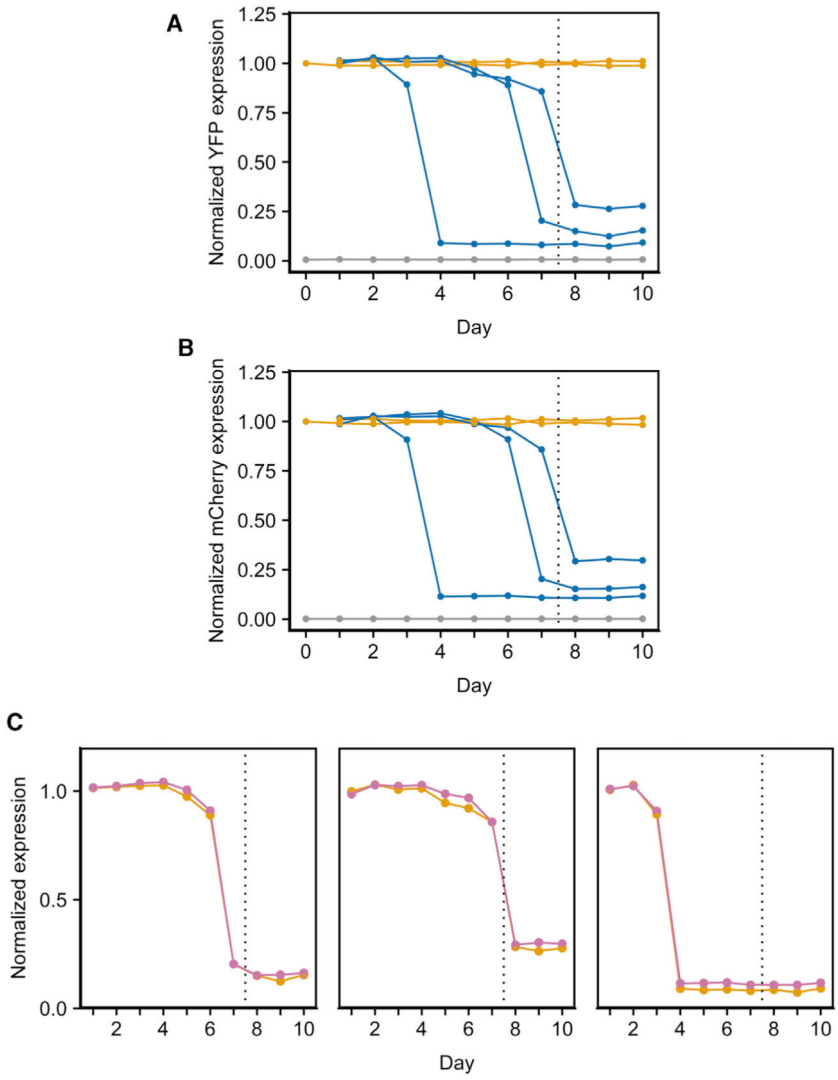

Figure 3. Expression Dynamics from the YFP-Sorting Experiment in WT Cells Containing P_{GAL1}-YFP and P_{GAL1}-mCherry

(A and B) Normalized YFP (A) and mCherry (B) expression levels from the YFP-sorting experiment in WT cells containing P_{GAL1}-YFP and P_{GAL1}-mCherry. Blue indicates samples sorted for the lowest expression, orange indicates positive control, and gray indicates negative control. The dashed line indicates the time at which expression-level-based sorting is terminated. All expression levels are normalized to the positive control.

(C) Comparison of YFP (orange) and mCherry (pink) expression-level trajectories of the three samples sorted for the lowest expression in (A) and (B). Each subpanel represents one sample. The dashed line indicates the time at which expression-level-based sorting is terminated. All expression levels are normalized to the positive control.

See also Figure S1.

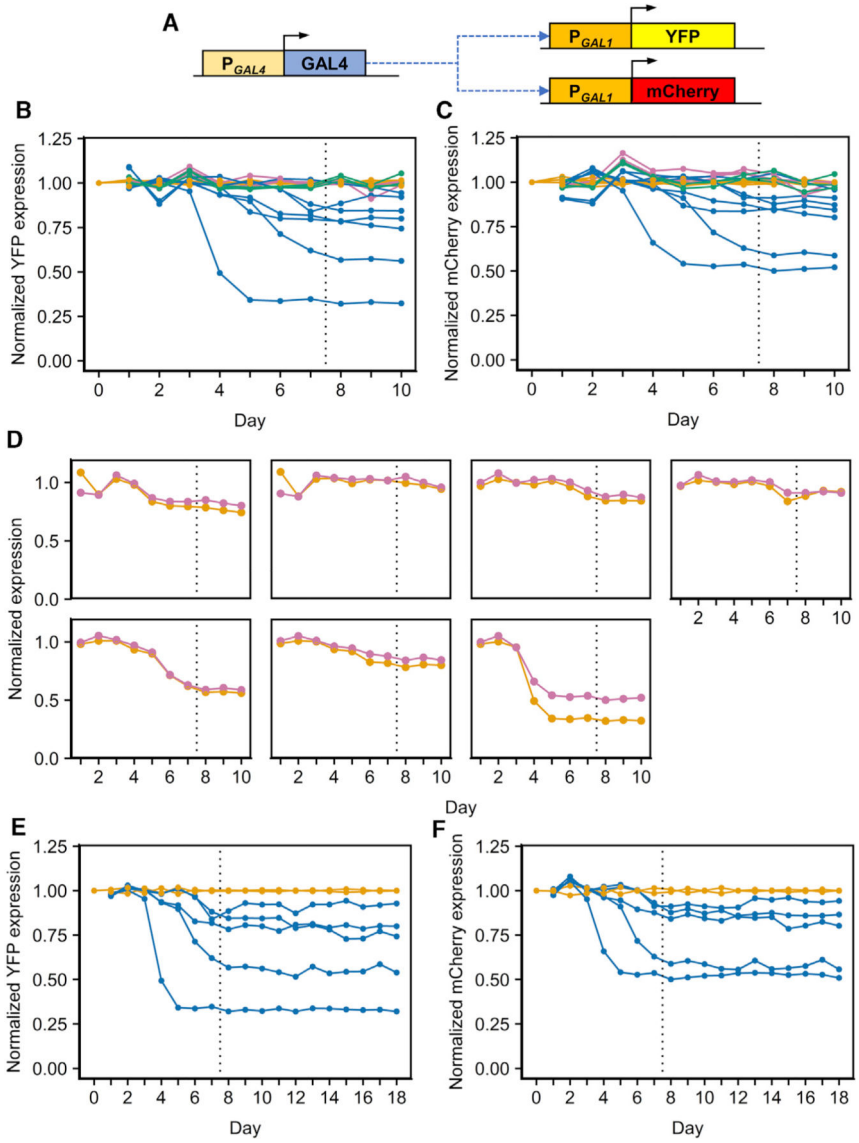

Figure 4. Dissecting System Behavior in the Constitutively Active GAL Network

(A) Gene network architecture of the *gal80Δ* strain.

(B and C) Normalized YFP (B) and mCherry (C) expression levels from the YFP-sorting experiment in *gal80Δ* cells. Pink indicates samples sorted for the highest expression, green indicates samples sorted for the median expression, blue indicates samples sorted for the lowest expression, and orange indicates positive control. The dashed line indicates the time at which expression-level-based sorting is terminated. All expression levels are normalized to the positive control.

(D) Comparison of YFP (orange) and mCherry (pink) expression-level trajectories of the nine samples sorted for the lowest YFP expression in *gal80Δ* cells. Each subpanel represents one sample. The dashed line indicates the time at which expression-level-based sorting is terminated. All expression levels are normalized to the positive control.

(E and F) Normalized YFP (E) and mCherry (F) expression levels from the extended YFP-sorting experiment in *gal80Δ* cells. Blue indicates samples sorted for the lowest expression,

and orange indicates positive control. The dashed line indicates the time at which expression-level-based sorting is terminated. All expression levels are normalized to the positive control.

See also Figures S2–S5 and Data S1, S2, S3, and S4.

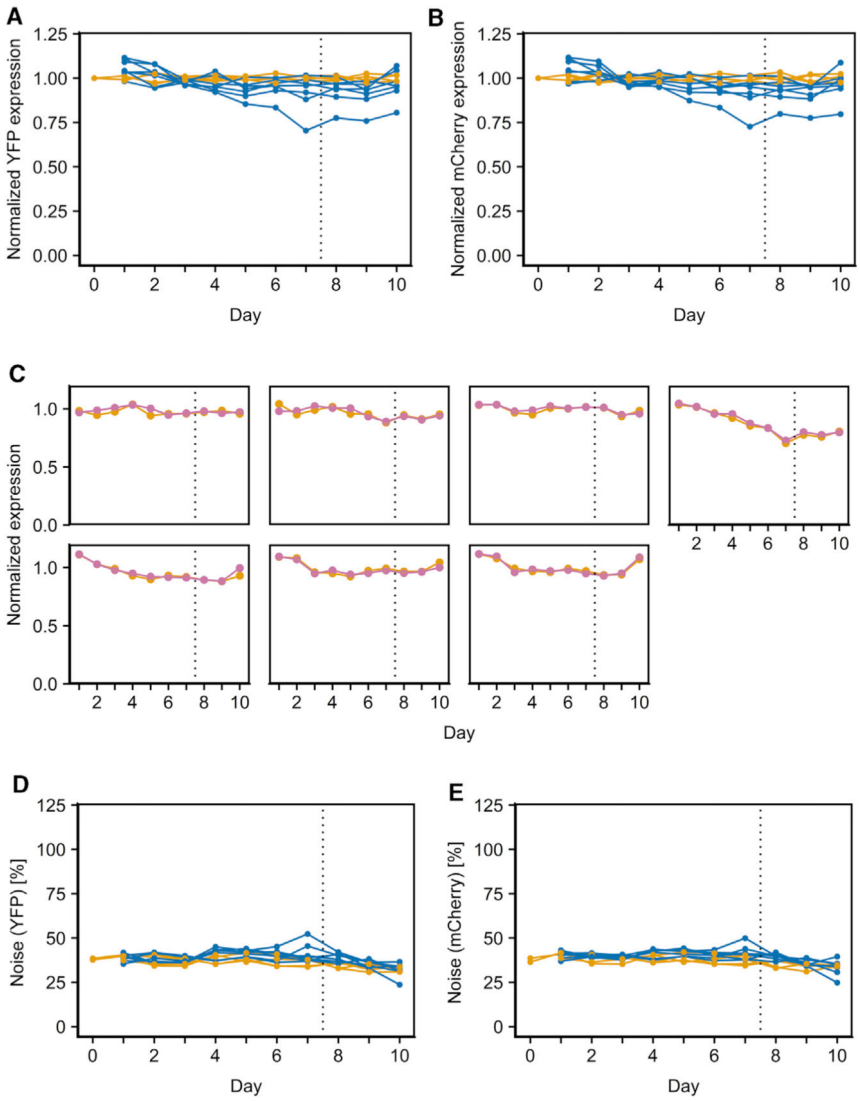

Figure 5. The Effect of the Local Chromatin Environment on Observed Results

(A and B) Normalized YFP (A) and mCherry (B) expression levels from the mCherry-sorting experiment in *gal80Δ* cells. Blue indicates samples sorted for the lowest expression, and orange indicates positive control. The dashed line indicates the time at which expression-level-based sorting is terminated. All expression levels are normalized to the positive control.

(C) Comparison of YFP (orange) and mCherry (pink) expression-level trajectories of the nine samples sorted for the lowest mCherry expression in *gal80Δ* cells. Each subpanel represents one sample. The dashed line indicates the time at which expression-level-based sorting is terminated. All expression levels are normalized to the positive control.

(D and E) Noise in YFP (D) and mCherry (E) expression levels from the mCherry-sorting experiment in *gal80Δ* cells. Blue indicates samples sorted for the lowest expression, and orange indicates positive control. The dashed line indicates the time at which expression-level-based sorting is terminated.

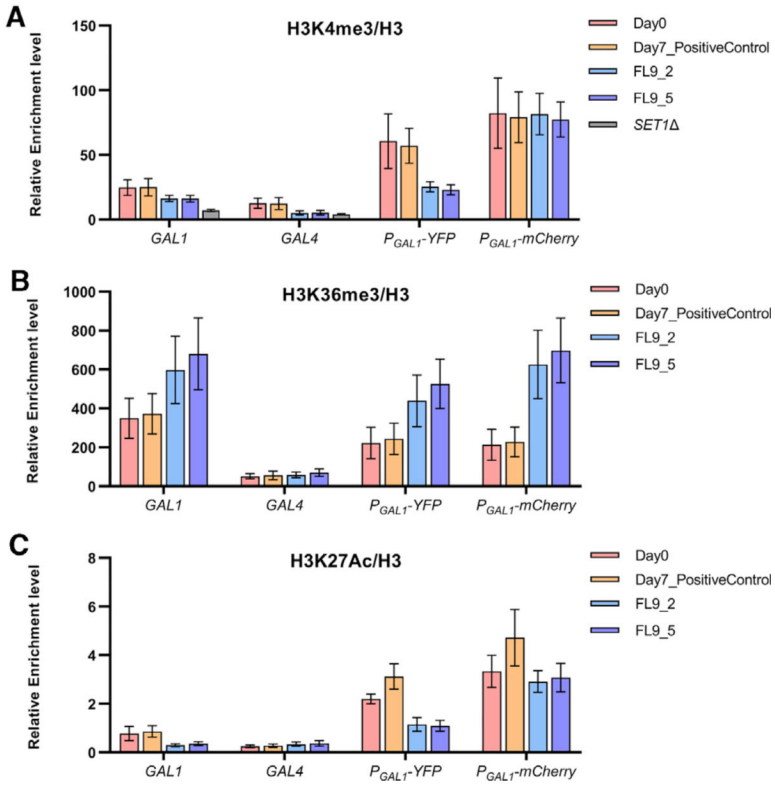

Figure 6. Epigenetic Modification Levels Quantified by ChIP-qPCR

Three types of epigenetic marks—H3K4me3 (A), H3K36me3 (B), and H3K27Ac (C)—were characterized at four genetic loci—*GAL1*, *GAL4*, P_{GAL1}-YFP, and P_{GAL1}-mCherry—in four isogenic populations: Day0, Day7 positive control, FL9_2, and FL9_5. An additional strain, *SET1*Δ, was included for H3K4me3 (A) as a technical control. Error bars indicate SEM (n = 4).

See also Figures S6 and S7 and Tables S1 and S2.

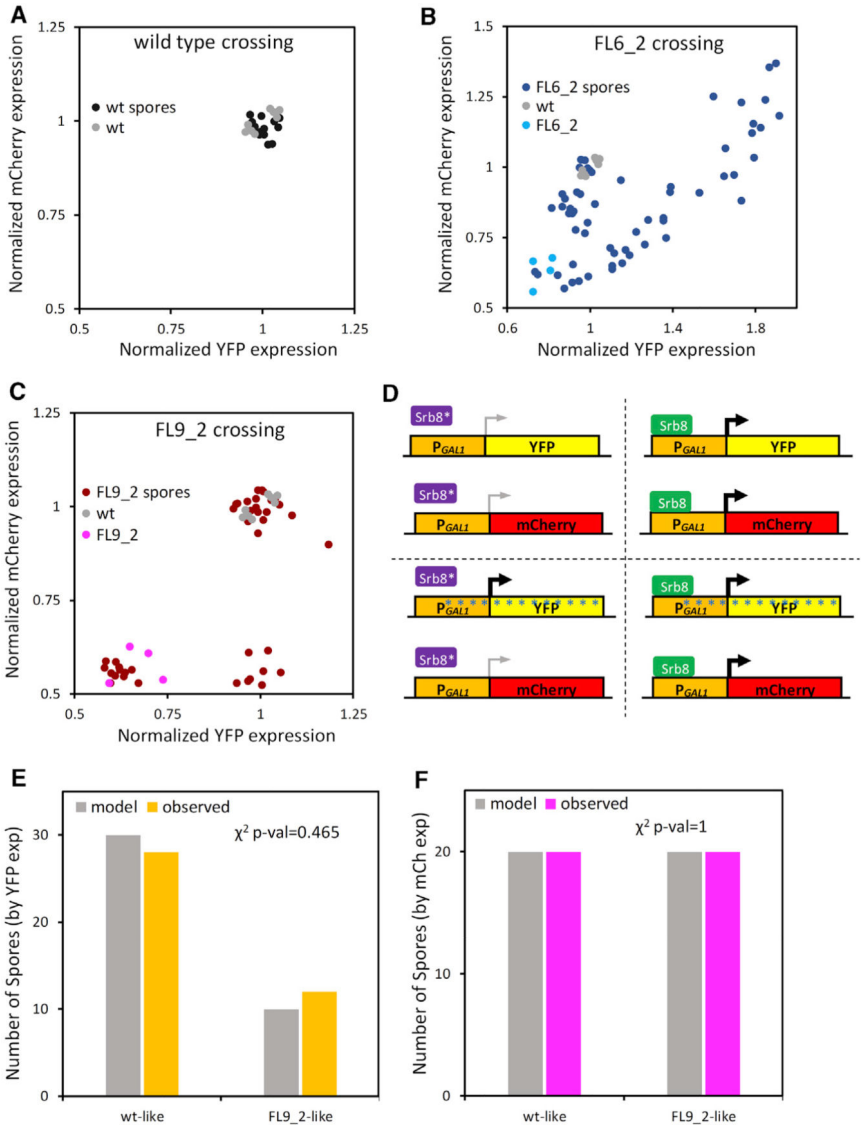

Figure 7. Sporulation-Based Assessment of Genetic versus Epigenetic Contributions on the Observed Phenotypes

(A–C) Scatterplot of the mean measured YFP and mCherry expression displayed by the spores coming from the WT-to-WT crossing (A), the FL6_2-to-WT crossing (B), and the FL9_2-to-WT crossing (C). The expression levels displayed by the parental strains are also shown.

(D) Proposed model explaining the expression distributions of the offspring obtained from the FL9_2-to-WT crossing. The purple Srb8* represents the mutated version identified by WGS, while the green Srb8 represents the WT version. The asterisks along the YFP locus represent the proposed epigenetic mark modulating reporter expression independently from the *SRB8* allele inherited. The color and width of the arrows indicate the strength of the gene expression (thin and gray, FL9_2-like low expression; thick and black, WT-like expression).

(E and F) Bar plots showing the number of spores displaying a given phenotype (WT-like or FL9_2-like), expected by the model and observed experimentally, for the YFP (E) and mCherry (F) expression phenotypes.

KEY RESOURCES TABLE

REAGENT or RESOURCE	SOURCE	IDENTIFIER
Antibodies		
α-H3K4me3	Abcam	Cat# ab8580; RRID:AB_306649
α-H3K36me3	Abcam	Cat# ab9050; RRID:AB_306966
α-H3Ac	Millipore	Cat# 07-360; RRID:AB_310550
α-H3	Abcam	Cat# ab1791; RRID:AB_302613
Experimental Models: Organisms/Strains		
S. cerevisiae: Strain background: W303 MATα	Our Lab Stocks	MA0001
S. cerevisiae: Strain background: W303 MATa	Our Lab Stocks	MA0002
S. cerevisiae: Strain background: W303 MATα ho::HIS5-P_{GAL1}-YFP	Our Lab Stocks	WP35
S. cerevisiae: Strain background: W303 MATα, ho::HIS5-P_{GAL1}-YFP, ura3::URA3-P_{GAL1}-mCherry	This paper	WP35URAPg1mC
S. cerevisiae: Strain background: W303 MATα, ho::HIS5-P_{GAL1}-YFP, ura3::URA3-P_{TEF1}-mCherry	This paper	WP35URAPtefmC
S. cerevisiae: Strain background: W303 MATα, ho::HIS5-P_{GAL1}-YFP, ura3::URA3-P_{GAL1}-mCherry, gal80Δ::NatNT2	This paper	XLUYmCgΔ80
S. cerevisiae: Strain background: W303 MATa, ho::HIS5-P_{GAL1}-YFP, ura3::URA3-P_{GAL1}-mCherry, gal80Δ::KanMX4	This paper	DMY375
Recombinant DNA		
Plasmid: pRS306	(Sikorski and Hieter, 1989)	N/A
Plasmid: pRS305	(Sikorski and Hieter, 1989)	N/A
Plasmid: pYM17	(Janke et al., 2004)	N/A
Plasmid: pFA6-kanMX4	(Wach et al., 1994)	N/A
Plasmid: HIS5-P_{GAL1}-YFP	Our Lab Stocks	N/A
Plasmid: URA3-P_{GAL1}-mCherry	This paper	N/A
Plasmid: URA3-P_{TEF1}-mCherry	This paper	N/A
Plasmid: pRS314-CAS9	Our Lab Stocks	N/A
Chemicals, Peptides, and Recombinant Proteins		
Gibson Assembly® Master Mix	New England BioLabs	E2611S
Restriction Enzyme: BstBI	New England BioLabs	R0519S
iTaqTM Universal SYBR® Green Supermix	Bio-Rad	1725120
Protein G-Sepharose	GE Healthcare	17-0618-01
Pronase	Roche	11 459 643 001
High Capacity RNA-to-cDNA kit	Applied Biosystems	4388950
YeaStar Genomic DNA Kit	ZYMO Research	D2002
Cycloheximide	Sigma-Aldrich	C7698
cOmplete protease inhibitor cocktail	Roche	11697498001
PMSF	AmericanBio	AB01620
β-glucuronidase	Sigma-Aldrich	G7017

REAGENT or RESOURCE	SOURCE	IDENTIFIER
Oligonucleotides		
Primers for qRT-PCR and ChIP-qPCR, see Table S2	This paper	N/A
Deposited Data		
GenBank: SAMN11440943	GenBank	N/A
GenBank: SAMN11440944	GenBank	N/A
GenBank: SAMN11440945	GenBank	N/A
GenBank: SAMN11440946	GenBank	N/A
GenBank: SAMN11440947	GenBank	N/A
GenBank: SAMN11440948	GenBank	N/A
GenBank: SAMN11440949	GenBank	N/A
GenBank: SAMN11440950	GenBank	N/A
Software and Algorithms		
NEBuilder® Assembly Tool	New England BioLabs	N/A
BD FACSuite	BD Biosciences	N/A
R	www.R-project.org	N/A
Bioconductor flowCore package	(Hahne et al., 2009)	N/A
Trimmomatic	(Bolger et al., 2014)	N/A
BWA-MEM	(Li, 2013)	N/A
Picard's MarkDuplicates	https://github.com/broadinstitute/picard	N/A
GATK tools	(Van der Auwera et al., 2013)	N/A
VCFtools	(Danecek et al., 2011)	N/A
VEP tool	(McLaren et al., 2016)	N/A
Other		
BD FACS-Aria	Becton Dickinson	N/A
Cary 60 UV-Vis Spectrometer	Agilent Technologies	N/A
Zeiss Tetrad "Advanced Yeast Dissection Microscope"	Carl Zeiss	N/A
Illumina HiSeq4000	Illumina	N/A